Technological and Environmental Prospects of Low Aspect Ratio Tokamak Reactor VECTOR

S. NISHIO[1)], K. TOBITA[1)], K. TOKIMATSU[2)], K. SHINYA[3)], I. SENDA[3)], T. ISONO[1)], Y. NAKAMURA[1)], M. SATO[1)], S. SAKURAI[1)], M. YAMAUCHI[1)], T. NISHITANI[1)], K. TANI[1)], S. SENGOKU[1)], Y. KUDO[1)], Y. SONG[1)], S. KONISHI[4)]

1)Naka Fusion Research Establishment, Japan Atomic Energy Research Institute, Naka-machi, Naka-gun, Ibaraki-ken, 311-0193 Japan, 2)Research Institute of Innovative Technology for the Earth, 3)Toshiba Corporation, 4)Kyoto University

e-mail contact of main author : nishio@naka.jaeri.go.jp

Abstract. Optimization of VECTOR design parameters has led to a fusion output of 2.5 GW with a small reactor weight of 8,800 tons. Current ramp-up simulation with TSC (Tokamak Simulation Code) demonstrated a stable current ramp-up with externally non-inductive current drive and bootstrap current when a central current is induced externally enough to avoid an extreme revesed shear such as current hole. It was numerically confirmed that such a low-A reactor would have an advantage of α-particle confinement. The divertor is designed to use a flux expansion of scrape-off-layer in the divertor region to maintain the heat flux on the divertor plate to be lower than 10 MW/m^2 without remote radiative cooling. Because of its compactness, CO_2 emission in a life cycle of a VECTOR power plant is estimated to be as low as 3.2 g-CO_2/kWh, being lower than that of an ITER-sized DEMO reactor (4.9 g-CO_2/kWh). As to the waste management of VECTOR, on the basis of reactor design and radiological considerations, we suggest reusing a liquid metal breeding material (PbLi) and neutron shield material (TiH_2) in successive reactors. Due to this waste management, its disposal waste would be reduced to as low as 3,000-4,000 tons, which is comparable with the radioactive waste of a light water reactor (4,000 tons in metal).

1. Introduction

Removing the center solenoid (CS) coil system from a conventional tokamak reactor concept, brings two major advantages. One of them is the lower aspect ratio, hence the plasma performances denoted by plasma elongation and plasma beta can be improved. Another one is that the toroidal field (TF) coil inner legs form a solid-like integrated center post (CP) structure. Hence, this configuration has a structural rigidity and the stored energy is relatively low in spite of its higher field strength. Under this background, an economical and compact reactor concept featuring the combination of low aspect ratio (A~2) and superconducting toroidal field coils [1] shown as VECTOR'02 in Fig.1. In VECTOR'02, a single null divertor (SND) configuration and A=2 were chosen. The SND configuration requires a relatively low plasma elongation of less than 2.0~2.1 to avoid the equilibrium bifurcation problem. For VECTOR'03 [2], new parameters have been optimized to maximize (fusion output) /(reactor weight) with feasible engineering and plasma parameters (Fig.1): $B_{max} \leq 19$ T, the neutron wall load $P_n \leq 5$ MW/m^2, Greenwald fraction $f_{GW} \leq 1$, confinement improvement factor HH ~ 1.2, normalized beta $\beta_N \leq 5.5$ and etc. As a result, we have reached an optimal design with plasma major radius R = 3.2 m, plasma minor radius a = 1.4 m, aspect ratio A = 2.3, plasma elongation κ = 2.35, plasma current I_p = 14 MA, bootstrap current fraction f_{bs} = 0.83 and fusion power P_{fus} = 2.5 GW. The reactor weight is reduced to 8,800 tons, a half or one third of the weight of other tokamak reactors.

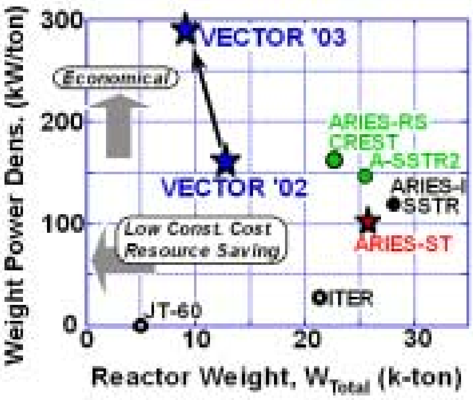

Fig. 1 Reactor weight and weight power density of VECTORs in comparison with conventional tokamak reactors.

In section 2, one of the key issues for a CS-less tokamak, i.e., the feasibily of plasma start-up and plasma current ramp-up are described. In section 3, α-particle loss induced by ripple transport is described. Section 4 describes the divertor heat loads. In section 5, VECTOR is evaluated from the viewpoint of a public acceptance. A summary is given in section 6.

2. Plasma start-up and current ramp-up

Plasma start-up and current ramp-up are the most important issue for the CS-less tokamak.

2.1 Plasma start-up

Even if the CS coil is removed, a toroidal electric field (one-turn voltage), but even a faint value can be achieved by a careful control of the another poloidal field (PF) coil currents with keeping a stray field less than a certain value and a RF pre-ionization power input. The plasma start-up (breakdown) is possible if ionization power rate exceeds the losses. For the plasma start-up provided by externally applied voltage, this condition is determined by the Townsent avalanche process.

The PF coil system of VECTOR can provide voltage $V_{loop} = 3V$ under the condition of less than ~1GW of the PFC power supply within a duration time Δt = 0.1s which could be used for the Townsent avalanche breakdown [3]. The stray field B_V is less than 10 Gauss with consideration of an eddy currents effects. On the other hand a field line connection length L denoted by

$$L = 0.25 a_{eff} (B_0 / B_V) \quad (1)$$

where a_{eff} and B_0 are an effective plasma minor radius for the breakdown process and the toroidal field strength at the breakdown region. The connection length L is evaluated to be little more than 1000 m. The minimal voltage V_{min} necessary to provide the breakdown is expressed as follow [3].

$$V_{min} = 2.5\mathrm{X}10^4 \pi R_p p_0 / ln(510 p_0 L) \quad (2)$$

Here R_P and p_0 are the plasma major radius and the pre-fill gas pressure, respectively. When the pre-fill gas pressure p_0 is in the range of $4\times10^{-6} \sim 1.5\times10^{-5}$ Torr which corresponds to the range of plasma density after the complete plasma ionization, the VECTOR PFC system can provide the necessary condition for the plasma breakdown.

2.2 Plasma current ramp-up

A new operational scenario of advanced tokamak formation has been demonstrated in the JT-60U tokamak [4], the LATE device [5] and etc. without the use of the CS coil system. These results open up a possibility to greatly improve its economic competitiveness [2, 6].

A fully non-inductive (NI) current ramp in JAERI-tokamak reactor concept VECTOR without center solenoids (CS) was demonstrated via axisymmetric MHD simulations using the Tokamak Simulation Code (TSC) [7]. An externally applied NI current more than 70 % of the plasma current ramps up the plasma current from 250 kA up to ~ 5 MA within 600 sec, in cooperation with a high bootstrap (BS) current more than 40 % of the plasma current. While deposition profile of the NI current was assumed to be fixed, internal transport barrier (ITB)-generated BS currents was taken into consideration such that the ITB foot was continually adapted in accordance with time-evolution of magnetic shear reversal that was monitored throughout TSC simulations [8].

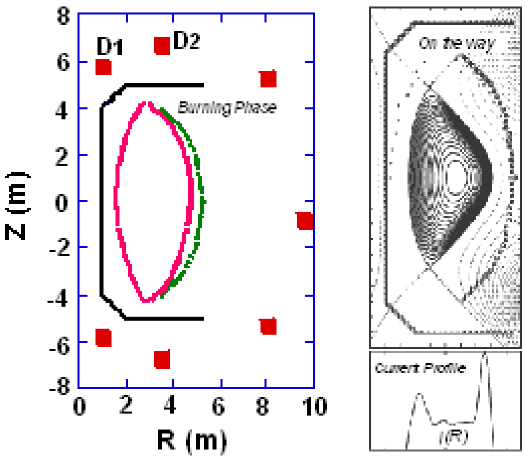

Fig. 2 Poloidal cross section of CS-less tokamak VECTOR with the so-called divertor coils D1 and D2. A typical equilibrium of negative magnetic shear plasma obtained by TSC simulation (t = 300 sec).

Figure 2 illustrates the VECTOR configuration

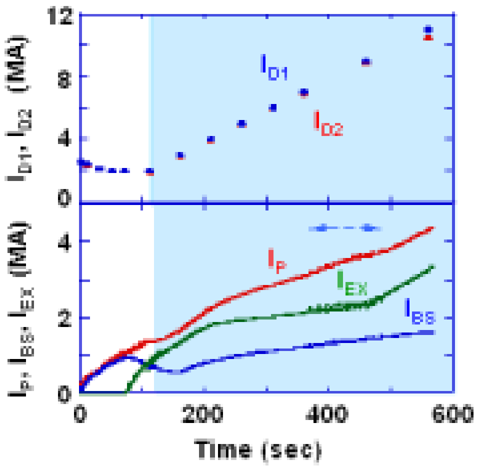

Fig. 3 TSC time-evolutions of the so-called divertor coil currents (I_{D1} and I_{D2}), plasma current (I_P), externally applied non-inductive current (I_{EX}) and bootstrap current (I_{BS}). The shadow region of later than 110 sec denotes a recharging phase for the so-called divertor coils. Notice the oscillatory behavior of plasma current specified by an arrow region due to non-linear link between BS current and magnetic shear profiles.

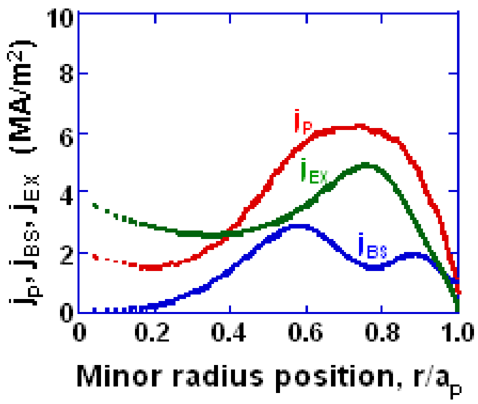

Fig. 4 Profiles of bootstrap, externally driven and total currents at t = 300 sec. Double humped wave pattern of BS current is due to formation of internal transport barrier.

with the so-called diverter coils D1 and D2, together with a typical TSC equilibrium of negative magnetic shear, diverted plasma at t = 300 sec. During the initial period of 110 sec, the so-called diverter coil currents of I_{D1} and I_{D2} were reduced to expand the plasma volume from limiter to diverter configuration, which is shown in Fig.3. Therefore, such discharging of the diverter coil current boosts the initial plasma current of 250 kA by a slight amount of inductive current less than 5 percent. During the following period of 110 – 600 sec, however, the diverter coil currents were contrarily recharged in order to suppress unfavorable further expansion of the plasma volume. Since the recharging of the diverter coil current acts against the plasma current ramp-up, a strong NI current drive I_{ni} is needed to increase the plasma current. Figure 3 shows that the TSC simulation of high BS current and strong NI current, which realizes an over driving state of plasma current almost over the entire plasma region, has successfully demonstrated a stable ramp-up of plasma current.

Notice the oscillatory ramp-up of plasma current during the period of 370 – 480 sec as specified by an arrow [9], where the relative fraction of the BS to NI currents becomes larger comparing with the other period. Figure 4 illustrates profiles of the BS, NI and total currents at t = 300 sec. Plenty of the ITB-generated BS current modifies the magnetic shear profile to cause an inward drift of the ITB region. When the ITB region is approaching the magnetic axis, the ITB structure disappears, and then the magnetic shear reversal jumps to an outer region. This cycle of the drifting and jumping process can be performed repeatedly, leading to a lowering of safety factor at the magnetic axis q_0. At the period later than 480 sec, the BS current fraction decreases, and then the oscillatory behavior ceased.

The TSC simulation has pointed out as follows: (1) In order to accelerate the ramp-up speed, electron temperature Te should be low to reduce return current as quickly as possible [10]. (2) Some amount of center drive of the NI current would be necessary to avoid a formation of current hole-like plasma configuration.

3. Confinement of α-particle

Numerical studies were carried out on toroidal-field (TF) ripple loss of α-particles using an orbit-following Monte-Carlo code [11]. In general, a low-A tokamak is expected to show reduced transport on α-particles. The aspect ratio dependence of the total power loss fraction of α-particles is heavily and shown in Fig.5. The following two factors are responsible for this.

(a) In low A, the TF ripple amplitude sharply damps along R in that the TF is mainly produced by the assembly of currents along the inner legs of the TF coils. Thus, the contribution of each TF coil becomes small compared with conventional values of A. This is seen in a model calculation of TF ripple distribution on the equatorial plane when 1% of the TF ripple amplitude is assumed at the outer plasma surface (Fig.6).

(b) In low A, trapped particles are less sensitive to TF ripple. This is because the impact of TF ripple is reduced by comparatively large $\partial B/\partial l$ on the low field side, where l stands for the length along the magnetic field line. This means that low A has a smaller ripple well domain and can show reduced ripple banana drift.

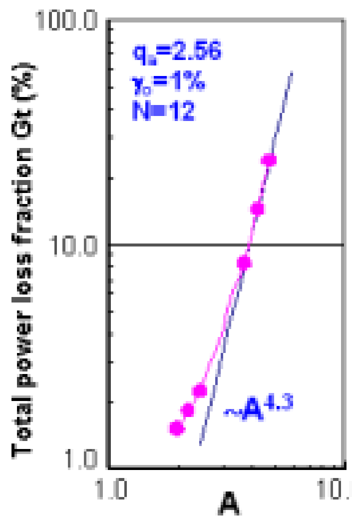

Fig. 5 Aspect ratio dependence of total power loss fraction of α-partyicles.

In fact, a simplified calculation, assuming a variation of only R with keeping the relative positions of plasma, first wall and TF coils and constant values of TF ripple at the outer plasma edge and the safety factor (q) at the plasma surface, indicates that the ripple loss decreases dramatically in low A [12]. In order to conclude on α-particle confinement in VECTOR, the OFMC calculations using more realistic MHD equilibrium. Because VECTOR has a high q compaered with conventional tokamak reactor, which tends to enhance the ripple loss, and the plasma shaping can affect the loss as well.

As summarized in ITER physics basis, α-particle ripple loss would be problematic in reversed shear plasma. Accordingly, to consider in an extreme case, the α-particle loss was calculated for a wide current hole [13]. Figure 7 depicts a numerical result for the α-particle loss fraction. The calculation was done using the parameters of two fusion reactors, VECTOR and A-SSTR2 [14]; A-SSTR2 is cited as a representative example (A= 4.1) of conventional tokamaks. Both cases assume the current hole radius of 0.6 and a broad birth profile of α-particles. Comparing at a same toroidal magnetic field (TF) ripple, low-A shows lower α-particle loss. From the point of view of the resulting peak heat load on the first wall, the allowable α-particle loss fraction is 2-3% for A-SSTR2, which is satisfied at the TF ripple of 0.3% at the plasma surface. In contrast, since the heat load distribution tends to expand and thus the peak heat load is reduced in low-A, higher α-particle loss fraction (~5%) is acceptable for VECTOR. As a result, the TF ripple of VECTOR can be designed at as high as 1.5% even for such a wide current hole.

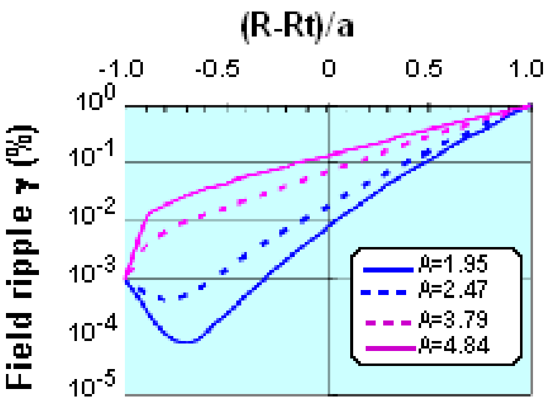

Fig. 6 Aspect-ratio dependence of field ripple profiles.

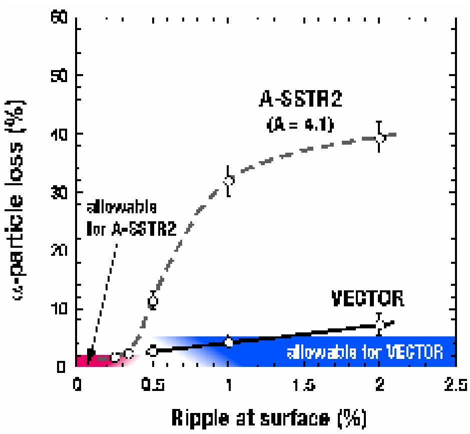

Fig. 7 Calculated α-paticle losses for a wide current hole plasma.

4. Divertor handling power

Conceptual case study was made on divertor power handling for a low aspect ratio tokamak reactor in this section. The conservative design path is explored to avoid uncertainty in the divertor plasma control. Divertor wetted (target) area for heat flux S_{tar} is important to maximize divertor handling power. Allowable power flow to inner and outer divertor plates P_{tar} can be written $q_{tar}S_{tar}=q_{tar}2\pi R_{div}\,\lambda_q^{mid}\,f_{tar}/\sin\theta_{tar}$ ($\lambda_q^{tar}=\lambda_q^{mid}\,f_{tar}$) as shown in Fig. 8 for the magnetic flux expansion between outer mid-plane SOL and divertor strike points f_{tar}. The heat flux width at outer mid-plane SOL λ_q^{mid} can be derived by the experience law for heat flux width for normal aspect ratio tokamaks[15]. Here, q_{tar} includes heat flux due to divertor radiation and should be less than 10MW/m^2 for the W mono-block armor with ferritic steel cooling pipe. Major radius of divertor R_{div} is determined by machine size and target angle θ_{tar} should be more then 15 degree for the margin to the alignment and fluctuation in plasma configuration. The minimum divertor leg length projected in a poloidal cross section $L_{div}^{Min}>2\lambda_q^{mid}f_{tar}/\tan\theta_{tar}+L_{rad}$ should be required to accept twice width of steady state heat load for the fluctuation in plasma configuration and broadening in ELM phase. In addition, inner divertor leg length is strongly limited by radial build at inboard side at the high triangularity and low aspect ration configuration, because inner divertor leg is straight forward to inboard wall in low triangularity configuration. Therefore, expanding magnetic flux tube and divertor wetted area requires long divertor leg length with low triangularity configuration for low aspect ratio. Comparison of power handling design for A=2.3 (δ_{95}=0), A=2.7 (δ_{95}~0.3) and A=3.0 (δ_{95}~0.3) are shown in table 1. It should be noted that divertor coil must be placed 11m apart from plasma center to obtain required divertor plasma configuration. Total radiation power at main plasma is assumed to be 200MW.

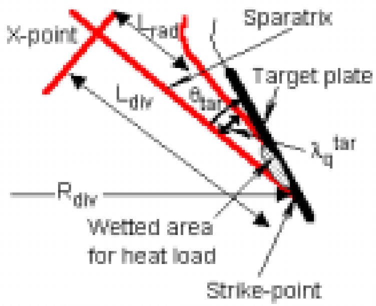

Fig. 8 Schematic drawing of field line configuration near the divertor plate.
R_{div} : major radius of strike point,
L_{div} : divertor leg length,
L_{rad} : radiative region length,
q_{tar} : angle between target plate and separatrix,
λ_q^{tar} : effective width of heat flux.

Table 1 Aspect ratio dependence on divertor power handling

Parameters	A=2.3	A=2.7	A=3.1
Major radius (m)	4.3	5.3	6.1
Toroidal field B_T (T)	4.6	5.3	6.3
Elongation κ_{95}	2.39	2.18	1.99
Triangularity δ_{95}	0.0	0.3	0.3
Safety factor q_{95}	5.3	4.9	4.6
Heatflux width λ_q^{mid} (mm)	31	28	24
α heating+P_{NBI} (MW)	696	690	685
Main radiation (MW)	200	200	200
Divertor geometry	(in/out)	(in/out)	(in/out)
Flux expansion f_{tar}	13/13	13/11	10/9
Leg length L_{div}(m)	2.7/2.7	1.6/2.5	1.5/1.9
Incident angle θ_{tar}(deg)	20/20	33/15	27/15
Target wetted area S_{tar}(m^2)	18/47	12/35	12/27
Steady state	(in/out)	(in/out)	(in/out)
Power to divertor P_{div} (MW)	**142/354**	**163/327**	**162/323**
Required radiation power density (MW/m^3)	**0/0**	**3.8/0**	**3.9/3.5**
type I ELM (S_{ELM} =1.5S_{tar})	(in/out)	(in/out)	(in/out)
Heat load q_{ELM} (MJ/m^2)	**1.3/0.5**	**2.1/0.7**	**1.8/0.8**

Heat flux width at SOL will be more than twice for that in ITER due to higher power to the SOL and higher safety factor and lower toroidal magnetic filed. The divertor handling power ≥500 MW can be obtained by expanding magnetic flux tube $f_{tar}\geq10$ with leg length ≥ 2m. No divertor radiative cooling required in low triangularity configuration. On the other hand, transient heat load due to type I ELM will be expected to exceed $1MJ/m^2$ for inner divertor by the scaling[16] with pedestal temperature of 5 keV. Reduction by type II ELM can be expected in high triangularity cases[17], but more expansion of wetted area should be required for low triangularity configuration.

5. Environmental impacts of VECTOR

5.1 Life cycle analysis

Using data on consumed materials for a conceptual design of VECTOR, life cycle analysis (LCA) was carried out [18]. The plant was assumed to include the power plant core (i.e., first wall, blanket, divertor, vacuum vessel, superconducting magnet coils, cryostat, and associated accessories) and primary/secondary cooling system (including compressor, evaporator, pump, turbine, motor-generator, water condensation, heat exchanger and pipe). Data regarding materials and energy required for buildings both of reactor and of turbine, plant site, decommissioning and disposal are assumed to the same as the assessment of light water reactor.

Life cycle CO_2 ($LCCO_2$) for VECTOR is as low as 3.2 gCO_2/kWh; 80% of which is due to consumed materials and energies for constructing the plant, and about 20% is due to replacenent of the blanket for plant operation. In comparison, $LCCO_2$ for an ITER-sized 1GW plant [19] is 4.9 gCO_2/kWh. This result indicates that a reduction of reactor weight decreases $LCCO_2$. However, from the point of view of CO_2 emmission reduction, the need for a compact fusion reactor is not underlined. It is because less than 5 gCO_2/kWh of $LCCO_2$ is small much enough to stabilize atomospheric CO_2 level. As a matter of fact, the resulting $LCCO_2$ for nuclear fusion is lower by far than those of other energy sources ; 903-1216 gCO_2/kWh for coal- fired, 26-192 gCO_2/kWh for photovoltaic, 39.5-71.2 gCO_2/kWh for wind, and 9.8-12.6 gCO_2/kWh for light water reactor using uranium enriched by ultracentrigugals.

5.2 Waste assessment

In the environmental aspect, pursuing a compact reactor is of importance in waste management. However, it should be noted that the significance of reducing reactor weight is to decrease the total amount of waste but that the amount of radioactive waste is less dependent of the total reactor weight. Considering these situations, we propose to design a fusion reactor suitable for reuse [20]. Promising reuse components are neutron shield and liquid metal tritium breeding material. In VECTOR, LiPb is used as the tritium breeding and neutron multiplying material. At the decommissioning, LiPb is collected in a storage tank to cool down the radioactivity. The contact dose rate of LiPb after the decommissioning decreases as time evolves, dropping to a remote recyclable level of ~10 mSv/h within 100 years. The dominant nuclides determining the contact dose rate are ^{207m}Pb and ^{207}Bi which originated from Pb. Since LiPb can be reused only by melting and simple composition control, a contact dose higher than 10 mSv/h may be acceptable for reuse. If 100 mSv/h is accepted, the required cooling time is about 2 years after decommissioning. VECTOR adopts TiH_2 as a sheld material. The neutron shield is composed of the assembly of steel (or SiC/SiC) containers filled with TiH_2. This is to confine powder TiH_2 in a rigid boundary and to avoid dissociation of hydrogen from TiH_2. The contact dose of TiH_2 decreases 10 mSv/h in 2 years after decommissioning. As to the neutron shield, the processes needed for installation to the next generation reactor are also expected to be simple, being suitable for reuse.

When the tritium breeding material and neutron shield are disposed in once through, the spent LiPb is classified as medium level waste (MLW) and most of the used shield must be disposed as mainly low level waste (LLW) and partly as MLW. Here, MLW is requiered deep land burial in disposal while LLW is qualified for shallow land burial. In the reuse, the components do not require complicated processes for reproduction, which make the economical and technological problems insignificant. Considering these aspects, there would be much merit in reusing tritium breeding material and neutron shield. Figure 9 shows the weights of disposal waste and reusable/recyclable waste, indicating that the minimum disposal waste is realized by the combination of waste management strategies: 1) reinforced shielding, 2) a compact reactor and 3) reuse of the breeding material and neutron shield. The weight of disposal waste would be reduced to as low as 1,685 t. The assessment does not include ports and supports because it is difficult to determine the amount of them in the conceptual design phase. However, if we assume that the radwaste from them is about 1,000 - 1,500 tons, the radwaste to be disposed in land is about 3,000-4,000 tons, which is comparable with the radwaste of LWR (4,000 tons in metal).

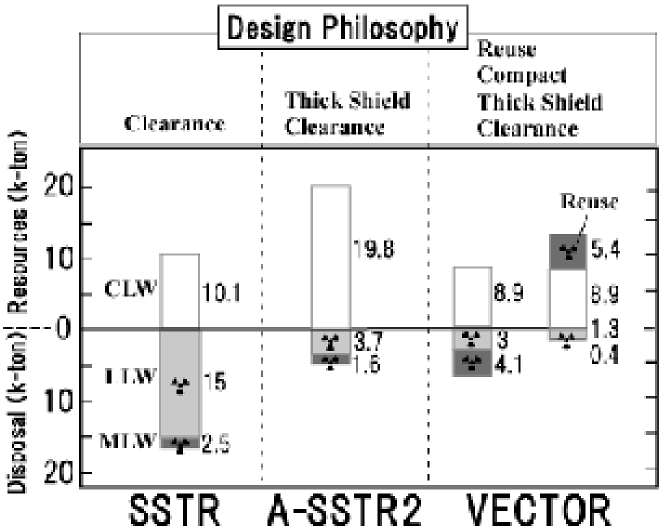

Fig.9 Classification of waste from SSTR, A-SSTR2 and VECTOR when various waste management strategies are introduced.

6. Summary

Recent design studies on VECTOR lead to the following results.

i) Parameters of VECTOR were optimized adopting a double null divertor with high elongation, leading to a reactor concept realizing a high power density (fusion output/ reactor weight = 2.3 GW/8,800 tons).

ii) TSC simulation based on the VECTOR configuration demonstrates a possibility of plasma current ramp-up without using CS coils.

iii) Numerical calculations using the OFMC code indicates that low-A tokamaks such as VECTOR have an advantage on α-particle ripple loss.

iv) In VECTOR, a problem on concentrated heat flux in the divertor due to its smallness in R seems to be dismissed using a flux expansion of SOL in the divertor.

v) To enhance a merit of compactness, we propose to reuse the used liquid breeder and shield of VECTOR to avoid the disposal of radwaste in land as possible. Assuming this waste management, the amount of disposal waste is assessed to be reduced to 3,000-4,000 tons, being comparable with the radwaste of LWR.

Acknowledgments

The authors are indebted to Profs. Y. Ono, Y. Takase, Y. Nagayama and T. Maekawa for information, suggestion, and discussion. The authors would like to acknowledge the beautiful CAD drawings provided by Ms. H. Hikita and the many graphs prepared by Mr. H. Shimane.

References

[1] S. Nishio *et al*., *Proc. 19th IAEA Fusion Energy Conf. (Lyon)* FTP1/21 (2002).
[2] S. Nishio, The papers of Technical Meeting on Plasma Science and Technology, IEE Japan, PST-03-37 (in Japanese), 10 Sep. 2003.
[3] ITER Physics Basis, Chapter 8, Nucl. Fusion **39** (1999) 2577.
[4] S. Shiraiwa, S. Ide, *et. al*., Phys. Rev. Lett. **92**, 035001 (2004).
[5] T. Maekawa *et al*., *Proc. 20th IAEA Fusion Energy Conf. (Vilamoura), EX/P4-27.*
[6] D. Moreau and I. Voitsekhovitch, Nucl. Fusion **39**, 685 (1999).
[7] S.C. Jardin, N. Pomphery and J. Delucia, J. Comput. Phys. **66**, 481 (1986).
[8] Y. Nakamura, *et. al*., J. Plasma & Fusion Res. SERIES Vol.6, accepted for publication.
[9] I. Voitsekhovitch and D. Moreau, Nucl. Fusion **41**, 845 (2001).
[10] S.C. Jardin, Nucl. Fusion **40**, 1101 (2000).
[11] K.Tani, et al., J.Phys.Soc.Jpn. **50**,1726-1737 (1981).
[12] K.Tani, et al.,Nucl. Fusion **33**,903-914 (1993).
[13] K.Tobita, et al., Plasma Phys. Controlled Fusion **46**, S95-S105 (2004).
[14] S. Nishio et al., J. Plasma and Fusion Research **78,** 1218 (2002).
[15] A. Loarte *et al*., J. Nucl. Mater. **266-269**, 587(1999).
[16] A. Loarte *et al*., J. Nucl. Mater. **313-316**, 962(2003).
[17] Y. Kamada *et al*., Plasma Phys. Contr. Fusion **42**, A247(2000).
[18] K. Tokimatsu and Y. Kaya., Role of Innovative Technologies for Global Energy and Environment, Proc. World Energy Congress, Sydney, 2004.
[19] S. Konishi et al*., Fusion Eng. Design* **63-64**, 11 (2002).
[20] K. Tobita et al., J. Nucl. Matter. **329-333**, 1610 (2004).